Gemini Multi-Object Spectrograph Observations of Scuba Galaxies Behind A851

M. J. Ledlow – Gemini Observatory, Chile
Ian Smail – University of Durham, UK
F. N. Owen – National Radio Astronomy Observatory, NM
W. C. Keel – University of Alabama
R. J. Ivison – Astronomy Technology Centre, Edinburgh, UK
G. E. Morrison – California Institute of Technology

Citation of published version:

Ledlow, M., Smail, I., Owen, F., Keel, W., Ivison, R., Morrison, G. (2002): Gemini Multi-Object Spectrograph Observations of Scuba Galaxies Behind A851. *The Astrophysical Journal Letters*, 577(2). DOI: 10.1086/344334

THE ASTROPHYSICAL JOURNAL, 577:L79–L82, 2002 October 1

GEMINI MULTI-OBJECT SPECTROGRAPH OBSERVATIONS OF SCUBA GALAXIES BEHIND A851

M. J. LEDLOW,[1] IAN SMAIL,[2] F. N. OWEN,[3] W. C. KEEL,[4] R. J. IVISON,[5] AND G. E. MORRISON[6]

Received 2002 June 21; accepted 2002 August 22; published 2002 September 3

ABSTRACT

We have identified counterparts to two submillimeter (submm) sources, SMM J09429+4659 and SMM J09431+4700, seen through the core of the $z = 0.41$ cluster A851. We employ deep 1.4 GHz observations and the far-infrared/radio correlation to refine the submm positions and then optical and near-infrared imaging to locate their counterparts. We identify an extremely red counterpart to SMM J09429+4659, while Gemini Multi-Object Spectrograph spectroscopy with Gemini North shows that the $R = 23.8$ radio source identified with SMM J09431+4700 is a hyperluminous infrared galaxy ($L_{\rm FIR} \sim 1.5 \times 10^{13}\ L_{\odot}$) at $z = 3.35$, the highest spectroscopic redshift so far for a galaxy discovered in the submm. The emission-line properties of this galaxy are characteristic of a narrow-line Seyfert 1 galaxy, although the lack of detected X-ray emission in a deep *XMM-Newton* observation suggests that the bulk of the luminosity of this galaxy is derived from massive star formation. We suggest that active nuclei, and the outflows they engender, may be an important part of the evolution of the brightest submm galaxies at high redshifts.

Subject headings: cosmology: observations — galaxies: evolution — galaxies: formation — galaxies: individual (SMM J09429+4659, SMM J09431+4700)

1. INTRODUCTION

Sensitive surveys in the submillimeter (submm) and millimeter wave bands have identified a population of distant dusty, active galaxies that may represent the formation phase of massive spheroidal galaxies (Smail, Ivison, & Blain 1997; Hughes et al. 1998; Bertoldi et al. 2000; Scott et al. 2002; Webb et al. 2002). Irrespective of the precise mechanism responsible for the prodigious luminosity of these galaxies, either star formation or dust-reprocessed radiation from an active galactic nucleus (AGN), several have been confirmed as high-redshift massive, gas-rich galaxies (Frayer et al. 1998, 1999). One of the most pressing issues for study is to identify the most distant examples. These provide a critical test of theoretical models of galaxy formation and evolution, which already struggle to produce sufficiently large gas masses in galaxies at $z \sim 2$ (Granato et al. 2002). Identifying similarly luminous, gas- and dust-rich mergers at even higher redshifts, $z > 3$, will provide even stronger constraints.

In this Letter, we discuss the identification and spectroscopic followup of two recently discovered submm galaxies in the field of the $z = 0.41$ cluster A851. Exploiting very deep radio and optical/near-infrared images, we identified counterparts to both submm sources and subsequently targeted them in spectroscopic observations with the Gemini Multi-Object Spectrograph (GMOS) on Gemini North. One of these galaxies has the highest spectroscopic redshift for a Submillimeter Common-User Bolometric Array (SCUBA) galaxy to date, at $z = 3.35$. We adopt a cosmology with $\Omega_m = 0.3$, $\Omega_\Lambda = 0.7$ and $H_0 = 70$ km s^{-1} Mpc^{-1}.

[1] Gemini Observatory, Southern Operations Center, AURA, Casilla 603, La Serena, Chile.

[2] Institute for Computational Cosmology, Department of Physics, University of Durham, South Road, Durham DH1 3LE, UK.

[3] National Radio Astronomy Observatory, P.O. Box O, Socorro, NM 87801. The NRAO is a facility of the National Science Foundation operated under cooperative agreement by Associated Universities, Inc.

[4] Department of Physics and Astronomy, University of Alabama at Tuscaloosa, Box 870324, Tuscaloosa, AL 35487.

[5] Astronomy Technology Centre, Royal Observatory, Blackford Hill, Edinburgh EH9 3HJ, UK.

[6] Infrared Processing and Analysis Center, California Institute of Technology, MS 100-22, Pasadena, CA 91125.

2. OBSERVATIONS AND REDUCTION

The two SCUBA galaxies discussed here were identified by Cowie, Barger, & Kneib (2002) in a deep 850 μm SCUBA map of A851 ($\sigma = 0.8$ mJy). These observations also detected SMM J09429+4658, previously cataloged and studied by Smail et al. (1999, 2002a). The two new sources are SMM J09431+4700 ($09^{\rm h}43^{\rm m}03\overset{\rm s}{.}96$, $+47°00'16\overset{''}{.}0$; all coordinates are J2000.0), which has an 850 μm flux density of 10.5 mJy, and SMM J09429+4659 ($09^{\rm h}42^{\rm m}53\overset{\rm s}{.}49$, $+46°59'52\overset{''}{.}0$) at 4.9 mJy. Cowie et al. (2002) use a detailed lens model for the cluster to estimate that these sources are likely to be amplified by a factor of 1.2 and 1.3 times, respectively.

The 1.4 GHz Very Large Array (VLA) map used in our analysis reaches a 1 σ noise level of 3.5 μJy beam^{-1} in the field center. Full details of the radio observations, their reduction, and cataloging are given in F. N. Owen et al. (2002, in preparation) and Smail et al. (2002b). The radio source surface density down to a 5 σ limit of 17.5 μJy is 4 arcmin^{-2} (Smail et al. 2002b). Adopting a nominal error radius of 3″ for the SCUBA sources (Smail et al. 2002a), this translates into only a 3% chance of an unrelated radio source falling within the SCUBA error circle. Searching within this radius around the position of SMM J09429+4659, we identify a bright, unresolved (<0″.15) 970 μJy radio source: H8 ($09^{\rm h}42^{\rm m}53\overset{\rm s}{.}42$, $+46°59'54\overset{''}{.}5$), 2″.5 from the submm position. For SMM J09431+4700, we identify two radio counterparts; one has a 1.4 GHz flux density of 72 μJy (H6: $09^{\rm h}43^{\rm m}04\overset{\rm s}{.}08$, $+47°00'16\overset{''}{.}2$) and is 1″.2 from the submm position, the other has 55 μJy (H7: $09^{\rm h}43^{\rm m}03\overset{\rm s}{.}70$, $+47°00'15\overset{''}{.}1$) and is 2″.8 away. The low surface density of radio sources suggests that H6 and H7 are both related to the submm emission. Both of these sources are slightly resolved in our VLA map, with sizes of 0″.7–0″.9.

We next exploit deep *BVRIzJHK* imaging of this field to identify the radio source counterparts of the submm galaxies in the optical and near-infrared. These images reach typical 3 σ depths of $m_{\rm AB} \sim 27$ in the optical and $m_{\rm AB} \sim 24$ in the near-infrared, and their reduction and calibration are described by Kodama et

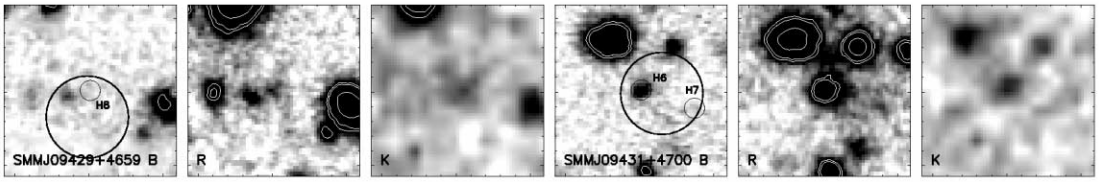

FIG. 1.—*BRK* views of the fields containing the submm sources SMM J09429+4659 and SMM J09431+4700. The large circles show the nominal 6″ diameter error circle for the SCUBA sources, while the smaller circles show the positions of the radio counterparts. Note the strong contrast between the optical/near-infrared colors of H6 and the extremely red object, H8. Each panel is 12″ × 12″, with north to the top and east to the left.

al. (2001) and Smail et al. (2002b). We astrometrically align the near-infrared images to the radio frame with a precision of 0.″32 rms using the positions of 90 sources detected in the two wave bands. This allows us to pinpoint near-infrared counterparts to the many faint radio sources in our VLA map.

All three of the radio counterparts to the SCUBA galaxies are identified in our optical or near-infrared data: H6 has $K = 20.2$ and $(R-K) = 3.59 \pm 0.16$, H7 is undetected in K but is coincident with an $R = 25.9$, $(R-K) \leq 4.6$ galaxy, and H8 has $K = 19.7$ and is extremely red, with $(R-K) = 5.5 \pm 0.3$. We show the optical/near-infrared images of these galaxies in Figure 1. Unfortunately, neither galaxy lies in the sparse *Hubble Space Telescope* mosaic of this field discussed by A. Dressler et al. (2002, in preparation) and only H6 is detected at sufficient signal-to-noise ratio in our good-seeing optical images to reliably measure its intrinsic FWHM: 0.″4 ± 0.″1.

The spectroscopy of these galaxies was attempted with the GMOS (Davies et al. 1997) on Gemini North. The target of this survey was faint radio galaxies, which are likely to lie at $z \sim 1$–4 (F. N. Owen et al. 2002, in preparation), and so we aimed for the widest possible wavelength coverage and the highest resolution to maximize the chance of detecting weak emission and absorption features in these optically faint galaxies. To accomplish this, we observed each mask twice, once with the B600 grating (centered at 4730 Å) and then with the R400 grating (centered at 7920 Å) to provide continuous spectral coverage from 3500 Å to 1 μm. The detectors were read out in 3 amplifier mode with 2 × 2 binning (along both the spatial and dispersion axes). The resulting pixel scale is 0.″145 pixel^{-1} with dispersions of 0.91 Å pixel^{-1} (B600) and 1.37 Å pixel^{-1} (R400). Slitlets of 1″ × 5″ were placed on each target, giving a resolution of 3–4 Å.

A multislit mask was designed for the center field in A851, which includes both submm sources. A total of 2.5 hr integration was obtained with each of the B600 and R400 gratings on the nights of 2002 March 14 and 15 in 0.″7–0.″8 seeing. These observations were reduced and calibrated in a standard manner using IRAF scripts. We used a CuAr lamp spectrum for wavelength calibration and removed any remaining offsets using bright skylines. The spectra were flux-calibrated with observations of Feige 34 (B600) and HZ 44 (R400) observed through a 1″ long slit. Both H6 and H8 were targeted in the same mask. H7's proximity to H6 precluded placing slitlets on both sources. From the observation of source H8 ($R = 25.2$), we are unable to either identify any features or detect the continuum. However, we do identify a series of strong emission lines in the spectrum of H6 shown in Figure 2.

Finally, we have retrieved the *XMM-Newton* X-ray image of this field from the public archive[7] to place limits on the hard X-ray emission from the submm sources. This image provides 49.4 ks of useful integration from the EPIC MOS1 and MOS2 cameras and allows us to place 3 σ limits of 0.9×10^{-15} and 1.3×10^{-15} ergs s^{-1} on the unabsorbed 2–10 keV fluxes of SMM J09429+4659 and SMM J09431+4700. Adopting a photon index of 1.7, these limits translate into 3 σ lower bounds on the submm X-ray spectral indices (Fabian et al. 2000) of greater than 1.23 and greater than 1.25, respectively.

3. ANALYSIS AND RESULTS

We identify several strong emission lines in the combined GMOS spectrum of H6 shown in Figure 2, including Lyα, N v, and C iv. Based on the wavelength of the narrow Lyα line, we estimate a redshift of $z = 3.349$, consistent with the

[7] This work is based on observations obtained with the *XMM-Newton*, an ESA science mission with instruments and contributions directly funded by ESA member states and the US (NASA).

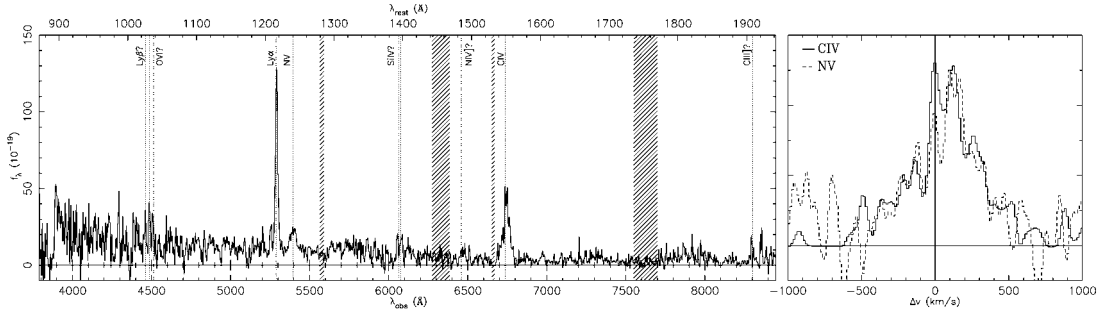

FIG. 2.—*Left*: GMOS spectrum of SMM J09431+4700, with the strongest features marked. The hatched regions indicate areas affected by detector features or atmospheric absorption or emission. The spectral properties of this galaxy are similar to those seen in NLSy1s. There are also hints of blueshifted absorption troughs on the stronger lines, although this is only tentative given the modest signal-to-noise ratio of our observations. *Right*: Comparison of the morphologies of the N v and C iv emission lines plotted on a rest-frame velocity scale relative to the redshift of the narrow Lyα line; the line centers are shown by the vertical solid line (the horizontal solid line indicates the continuum level). The matches between the different components probably reflects structure in the emission region. A 30 km s^{-1} shift to the blue has been applied to the N v line; this is within the relative calibration error of the red and blue spectra. To aid this comparison, both spectra have been smoothed to the instrumental resolution with a 3 Å FWHM Gaussian.

observed wavelengths of the other broader emission features. This is currently the highest spectroscopic redshift for the counterpart of a SCUBA galaxy—breaking the $z = 3$ barrier for this population for the first time. While this is only a modest increase in look-back time, compared to the previously most distant source at $z = 2.80$, it corresponds to a decrease of a factor of 2 in the predicted abundance of the massive halos, greater than $10^{12}\ M_{\odot}$, believed to host these luminous galaxies (Jenkins et al. 2001). The exponential decline in the space density of the most massive halos at higher redshifts underlines the strong constraints available from identifying the highest redshift submm galaxies.

The 850 μm flux of SMM J09431+4700 of 8.8 mJy (corrected for lensing) translates into $L_{\rm FIR} \sim 1.5 \times 10^{13}\ L_{\odot}$, assuming $T_d = 38$ K.[8] This makes this galaxy a hyperluminous infrared galaxy (HyLIRG; Rowan-Robinson 2000). If purely powered by massive star formation, its immense luminosity would require a star formation rate of $\sim 10^4\ M_{\odot}\ {\rm yr}^{-1}$!

However, the spectrum of H6 shows the signatures of a weak AGN. The strongest lines include a narrow and symmetrical Lyα line with a flux of 1.9×10^{-16} ergs s^{-1} cm^{-2} and a full width at zero intensity (FWZI) of 55 Å. There are also broader emission lines coincident with the expected wavelength of redshifted N v λ1239.7, with an observed FWZI of $\sim$155 Å and an integrated flux of $\sim 0.7 \times 10^{-16}$ ergs s^{-1} cm^{-2}, and C iv λ1549, with an FWZI of $\sim$173 Å and a flux of 2.1×10^{-16} ergs s^{-1} cm^{-2}. We also identify a number of weaker emission lines and mark these in Figure 2. The velocity widths of these lines cover a wide range, from a rest-frame FWHM of 210 km s^{-1} for Lyα up to $\sim$550 km s^{-1} for the higher excitation lines. In addition, the morphologies of the N v and C iv lines appear very similar (Fig. 2). The spectral properties, line widths, and line ratios of this galaxy are very similar to those seen for narrow-line Seyfert 1 galaxies (NLSy1s; Osterbrock & Pogge 1985; Crenshaw et al. 1991), in particular Mrk 24. This classification is supported by the ratio He ii λ1640/C iv = 0.05, indicative of an NLSy1 or narrow-line quasi-stellar object (Heckman et al. 1995). These galaxies have narrow forbidden and permitted emission lines, FWHM $\lesssim$400–700 km s^{-1}, which are thought to result from an increase in the size and density of the broad-line region compared to a normal Seyfert 1 galaxy (Laor et al. 1997).

Based on our deep imaging, we measure 3″ diameter photometry of H6, giving: $B = 25.82 \pm 0.07$, $V = 24.11 \pm 0.03$, $R = 24.00 \pm 0.03$, $I = 23.62 \pm 0.07$, $z > 24.1$ (3 σ), $J > 22.7$ (3 σ), $H = 21.41 \pm 0.25$, and $K = 20.41 \pm 0.14$. The $(B-V)$ color is relatively red, $(B-V) = 1.7$, suggesting the presence of either strong absorption in the B band or strong emission in the V band. We note that at $z = 3.35$ the Lyman limit falls just blueward of the B band (indeed emission is seen down to 890 Å in the rest frame, rising as $\lambda^{-2.5}$); however, several strong lines fall in the V band (Fig. 2). Integrating all the flux in the V-band part of the GMOS spectrum, we measure a slit magnitude of $V \sim 24.4$, in reasonable agreement with the 3″ diameter aperture magnitude, and from this we estimate that 50% of the V-band light is contributed by Lyα and N v; a similar calculation for C iv suggests that it contributes 35% of the R-band flux. Using the apparent K-band magnitude of this galaxy, we estimate an absolute V-band magnitude of $M_V \sim -23.0$ at $z = 3.35$, although a significant fraction of this light may be contributed by emission lines, including Hβ and [O iii] $\lambda\lambda$4959, 5007.

[8] If *both* H6 and H7 contribute to the submm emission, then from their joint radio flux we would estimate a somewhat higher dust temperature, $T_d = 49$ K, and a far-infrared luminosity of $L_{\rm FIR} = 3.6 \times 10^{13}\ L_{\odot}$.

We also investigate the spatial extent of the emission lines along our slit—focusing on Lyα and N v, as these lines lie close in wavelength. We find that Lyα is spatially extended compared to N v with an FWHM of 0.″95 versus 0.″74. As the estimated image quality in the r band was 0.″7 at the beginning of the observations, the N v width is consistent with being spatially unresolved. For Lyα, we measure an intrinsic FWHM of $\sim$0.″6—indicating extended Lyα emission on a scale of 8 kpc.

Turning to the radio properties of this galaxy, the radio luminosity of H6 is 5×10^{24} W Hz^{-1} for an $\alpha = -1$ spectral slope or 2.5×10^{24} W Hz^{-1} for $\alpha = -0.7$ (including a 20% correction for lensing). These luminosities correspond locally to those expected for an FR I radio galaxy, although it is equally consistent with strong radio emission from a massive starburst at the level detected in the submm wave band. The radio-submm spectral index, $\alpha_{1.4}^{850}$, is 0.91 ± 0.04 based on the radio emission from H6 (if H7 contributes as well, then $\alpha_{1.4}^{850} \sim 0.80$). These correspond to a redshift of $z = 2.7^{+1.7}_{-0.9}$ using the models from Carilli & Yun (2000), in reasonable agreement with our spectroscopic measurement.[9]

The *XMM-Newton* observations suggest that unless highly obscured, the intrinsic luminosity of the AGN in H6 must be modest, $L_{\rm X}(2\text{–}10\ {\rm keV}) \lesssim 10^{42}$ ergs s^{-1}. However, the limit on the submm X-ray spectral index of H6, greater than 1.25, is also consistent with a heavily obscured AGN such as NGC 6240 (Keel 1990), with $N({\rm H\ I}) \sim 10^{24}$, at $z = 3.35$ (Fabian et al. 2000).

4. DISCUSSION AND CONCLUSIONS

The spectroscopic identification of a second HyLIRG in the SCUBA population provides the opportunity for a detailed comparison of the properties of these two galaxies: SMM J02399−0136 and SMM J09431+4700. Detailed study of SMM J02399−0136 has shown that it is a massive, gas-rich system (Ivison et al. 1998; Frayer et al. 1998), identified with a pair of galaxies, L1 and L2, at $z = 2.80$, and has a far-infrared luminosity of $L_{\rm FIR} \sim 1 \times 10^{13}\ L_{\odot}$. L1 hosts a partially obscured AGN, which has recently been classified as a broad absorption line quasi-stellar object (BALQSO; Vernet & Cimatti 2001). The second component, L2, is separated from L1 by about 10 kpc in projection (compared to 50 kpc for H6–H7) and may be tidal debris rather than an independent galaxy.

Apart from their apparent binary morphologies, the most striking similarity between these two HyLIRGs is that both systems host AGNs. As highlighted by Ivison et al. (2000), 80% of the SCUBA galaxies with known redshifts show some signs of an AGN. The close relationship of AGN and QSO activity to the growth of supermassive black holes (SMBHs) and the apparent ubiquity of SMBHs in local, massive spheroids suggests that this is a natural consequence if SCUBA galaxies are the progenitors of the most massive galaxies in the local universe (e.g., Sanders et al. 1988; Silk & Rees 1998; Granato et al. 2001; Archibald et al. 2001). One measure of the importance of the AGN in these systems is to quantify its contribution to their total emission. X-ray observations of the two hyperluminous infrared submm galaxies suggests that in neither does the AGN dominate the bolometric emission (Bautz

[9] For the extremely red object/millijansky radio counterpart to SMM J09429+4659, H8, we estimate $\alpha_{1.4}^{850} = 0.30 \pm 0.07$, corresponding to only $z = 0.4 \pm 0.3$. It is clear that the radio emission must include a significant contribution from an AGN and the estimated redshift is only a lower limit—assuming the galaxy follows the K-z relationship for powerful radio galaxies, it most likely lies at $z \gtrsim 2$ (Jarvis et al. 2001).

et al. 2000), which instead comes from an intense starburst that also produces the substantial masses of dust in these galaxies.

Although they do not dominate the energetics, the AGNs may still have a profound effect on the evolution of these galaxies: the AGN in SMM J02399−0136 is driving a substantial wind, which may in time sweep the central regions of the galaxy clear of gas and dust. Can we find any signs of similar AGN-induced feedback in SMM J09431+4700? There are several hints: the contrast between the narrow, spatially extended Lyα emission and the broader but spatially unresolved high-excitation lines may indicate that the former arises from emission in an outflow. This situation is very similar to that seen in some high-redshift radio galaxies, such as 53W002 at $z = 2.4$ (Windhorst, Keel, & Pascarelle 1998). Moreover, the structured broad emission lines seen in H6 are reminiscent of the structures seen in broad emission lines of some radio galaxies and radio-loud QSOs (Eracleous & Halpern 1994), although those show much larger velocity ranges. These structured emission lines are interpreted as resulting from scattering of radiation from the AGN by outflowing conical winds (Corbett et al. 1998), and the same mechanism may be operating in SMM J09431+4700/H6. The final connection is from the spectral classification of this galaxy as an NLSy1, where analysis of examples at $z \sim 0$ have led to the identification of strong nuclear winds and a suggested link to BALQSOs (Lawrence et al. 1997; Leighly et al. 1997; Laor et al. 1997).

If both systems do show signatures of massive outflows, this suggests that winds powered by the AGNs (as well as starbursts) must be central to our understanding the growth of the spheroidal components in these massive, young galaxies (Granato et al. 2002). The feedback on the system from energy injected by the AGN provides one possible mechanism for creating the observed SMBH-to-bulge mass correlation seen in local galaxies (Maggorian et al. 1998). The future evolution of these submm sources will be determined by the ability of the AGNs to clear the bulk of the gas and dust from the nuclear regions—if they can, then they may evolve into the population of less obscured QSOs.

With regard to the wider environment of H6, we note a striking coincidence: H6 is just 400 km s^{-1} and less than 1 Mpc (64″) from an optically selected galaxy, DG 433 ($z = 3.3435$; Trager et al. 1997), suggesting that the two galaxies inhabit a single structure. DG 433 has a UV spectrum dominated by absorption lines and an estimated star formation rate of $\lesssim 10^2\ M_\odot\ \mathrm{yr}^{-1}$, indicating it is a much less active system than the hyperluminous galaxy H6. The relationship between the highly obscured and very active submm-luminous galaxies and the less obscured populations that cluster in the same environments will be one of the most important questions to address in the next few years.

This work is based on observations obtained at the Gemini Observatory, which is operated by the Association of Universities for Research in Astronomy, Inc., under a cooperative agreement with the NSF on behalf of the Gemini partnership: the National Science Foundation (US), the Particle Physics and Astronomy Research Council (UK), the National Research Council (Canada), CONICYT (Chile), the Australian Research Council (Australia), CNPq (Brazil), and CONICET (Argentina). We thank Taddy Kodama for the use of his exquisite Subaru imaging and an anonymous referee for helpful comments. We also thank Andrew Blain, Chris Carilli, Scott Chapman, Len Cowie, Chris Done, Alastair Edge, Inger Jorgensen, Jean-Paul Kneib, Rowena Malbon, Bryan Miller, Matt Page, and Graham Smith for useful discussions and help. I. S. acknowledges support from Royal Society and Philip Leverhulme Prize Fellowships.

REFERENCES

Archibald, E. N., Dunlop, J. S., Hughes, D. H., Rawlings, S., Eales, S. A., & Ivison, R. J. 2001, MNRAS, 323, 417
Bautz, M. W., Malm, M. R., Baganoff, F. K., Ricker, G. R., Canizares, C. R., Brandt, W. N., Hornschemeier, A. E., & Garmire, G. P. 2000, ApJ, 543, L119
Bertoldi, F., et al. 2000, A&A, 360, 92
Carilli, C. L., & Yun, M. S. 2000, ApJ, 530, 618
Corbett, E. A., Robinson, A., Axon, D. J., Young, S., & Hough, J. H. 1998, MNRAS, 296, 721
Cowie, L. L., Barger, A., & Kneib, J.-P. 2002, AJ, 123, 2197
Crenshaw, D. M., Peterson, B. M., Korista, K. T., Wagner, R. M., & Aufdenberg, J. P. 1991, AJ, 101, 1202
Davies, R. L., et al. 1997, Proc. SPIE, 2871, 1099
Eracleous, M., & Halpern, J. P. 1994, ApJS, 90, 1
Fabian, A. C., et al. 2000, MNRAS, 315, L8
Frayer, D. T., Ivison, R. J., Scoville, N. Z., Yun, M., Evans, A. S., Smail, I., Blain, A. W., & Kneib, J.-P. 1998, ApJ, 506, L7
Frayer, D. T., et al. 1999, ApJ, 514, L13
Granato, G. L., De Zotti, G., Silva, L., Danese, L., & Magliocchetti, M. 2002, Ap&SS, 281, 497
Granato, G. L., Silva, L., Monaco, P., Panuzzo, P., Salucci, P., De Zotti, G., & Danese, L. 2001, MNRAS, 324, 757
Heckman, T., et al. 1995, ApJ, 452, 549
Hughes, D. H., et al. 1998, Nature, 394, 241
Ivison, R. J., Smail, I., Barger, A., Kneib, J.-P., Blain, A. W., Owen, F. N., Kerr, T. H., & Cowie, L. L. 2000, MNRAS, 315, 209
Ivison, R. J., Smail, I., Le Borgne, J.-F., Blain, A. W., Kneib, J.-P., Bézecourt, J., Kerr, T. H., & Davies, J. K. 1998, MNRAS, 298, 583
Jarvis, M., et al. 2001, MNRAS, 326, 1563
Jenkins, A., Frenk, C. S., White, S. D. M., Colberg, J. M., Cole, S., Evrard, A. E., Couchman, H. M. P., & Yoshida, N. 2001, MNRAS, 321, 372
Keel, W. C. 1990, AJ, 100, 356
Kodama, T., Smail, I., Nakata, F., Okamura, S., & Bower, R. G. 2001, ApJ, 562, L9
Laor, A., Jannuzi, B. T., Green, R. F., & Boroson, T. A. 1997, ApJ, 489, 656
Lawrence, A., Elvis, M., Wilkes, B. J., McHardy, I., & Brandt, N. 1997, MNRAS, 285, 879
Leighly, K. M., Mushotzky, R. F., Nandra, K., & Forster, K. 1997, ApJ, 489, L25
Magorrian, J., et al. 1998, AJ, 115, 2285
Osterbrock, D. E., & Pogge, R. W. 1985, ApJ, 297, 166
Rowan-Robinson, M. 2000, MNRAS, 316, 885
Sanders, D. B., Soifer, B. T., Elias, J. H., Neugebauer, G., & Matthews, K. 1988, ApJ, 328, L35
Scott, S. E., et al. 2002, MNRAS, 331, 817
Silk, J., & Rees, M. J. 1998, A&A, 331, L1
Smail, I., Ivison, R. J., & Blain, A. W. 1997, ApJ, 490, L5
Smail, I., Ivison, R. J., Blain, A. W., & Kneib, J.-P. 2002a, MNRAS, 331, 495
Smail, I., Ivison, R. J., Kneib, J.-P., Cowie, L. L., Blain, A. W., Barger, A. J., Owen, F. N., & Morrison, G. 1999, MNRAS, 308, 1061
Smail, I., Owen, F. N., Morrison, G. E., Keel, W. C., Ivison, R. J., & Ledlow, M. J 2002b, ApJ, in press
Trager, S. C., Faber, S. M., Dressler, A., & Oemler, A. 1997, ApJ, 485, 92
Vernet, J., & Cimatti, A. 2001, A&A, 380, 409
Webb, T., et al. 2002, ApJ, submitted
Windhorst, R. A., Keel, W. C., & Pascarelle, S. M. 1998, ApJ, 494, L27